

Measurement-Induced Macroscopic Superposition States in Cavity Optomechanics

Ulrich B. Hoff,^{1,2,*} Johann Kollath-Bönig,¹ Jonas S. Neergaard-Nielsen,¹ and Ulrik L. Andersen¹

¹*Department of Physics, Technical University of Denmark, Building 309, 2800 Kongens Lyngby, Denmark*

²*Australian Research Council Centre of Excellence for Engineered Quantum Systems (EQuS), School of Mathematics and Physics, The University of Queensland, St. Lucia QLD 4072, Australia*

(Received 22 January 2016; published 28 September 2016)

A novel protocol for generating quantum superpositions of macroscopically distinct states of a bulk mechanical oscillator is proposed, compatible with existing optomechanical devices operating in the bad-cavity limit. By combining a pulsed optomechanical quantum nondemolition (QND) interaction with nonclassical optical resources and measurement-induced feedback, the need for strong single-photon coupling is avoided. We outline a three-pulse sequence of QND interactions encompassing squeezing-enhanced cooling by measurement, state preparation, and tomography.

DOI: [10.1103/PhysRevLett.117.143601](https://doi.org/10.1103/PhysRevLett.117.143601)

Introduction.—Elusive as they are, Schrödinger cat [1] states remain some of the hardest to tame in the quantum world, yet also among the ones most strived for. That is due to their quintessential embodiment of the manifestly nonclassical properties of quantum mechanics, by simultaneously occupying two macroscopically distinct states—dead *and* alive. Successful creation of such coherent state superpositions have so far been limited exclusively to isolated microscopic quantum systems, e.g. in ion traps [2,3] and microwave cavity and circuit quantum electrodynamics [4–7], while closely related variants, colloquially termed Schrödinger kittens, have been demonstrated in propagating optical fields [8–10]. However, an intriguing and long-standing question is whether also macroscopic objects can be prepared in quantum superpositions of being here *and* there?

A vast number of proposals for optomechanical generation of non-Gaussian mechanical states, such as cat states, exist in the literature [11–16]. Non-Gaussian states of light can be directly mapped onto the mechanical motional states either via a swapping operation [17–19] or by teleportation [20,21], but this can be achieved only in the highly challenging sideband resolved regime in which the mechanical frequency lies outside the resonance of a narrow-banded cavity (good cavity limit). Mechanical non-Gaussian states can also be generated in the much simpler bad cavity regime (where the sidebands are unresolved) by using a broadband cavity and either single photon [22] or coherent state resources [23]. However, these protocols rely on an extremely strong non-Gaussian interaction between light and mechanics and are thus of limited practical feasibility due to the insufficient optomechanical interaction strengths currently achievable.

As suggested in recent works [24–27], quantum nondemolition (QND) state transfer [28,29] induced by pulsed optomechanical interaction [30–32] offers a more feasible route. Extending this framework, we propose a novel squeezing-enhanced protocol for preparation of macroscopic

superposition states, using pulsed QND transfer of an optical catlike state onto a mechanical oscillator. The proposed scheme relies on the easily accessible sideband unresolved regime, the required optomechanical single-photon coupling strength being weak, and the resulting phase space separation of the constituent cat state components being large. We find that by using experimentally feasible system parameters, a superposition state of a massive system with a large degree of macroscopicity can be formed.

The core of the scheme is presented in Fig. 1. Vacuum squeezed light with squeezing parameter r impinges on an asymmetric beam splitter with transmission $T_{\text{tap}} \approx 1$, and a pulsed photon subtracted squeezed vacuum (PSSV) state [33] is conditionally prepared by photon number resolved detection with efficiency η on the tap-off. Such states can reach high levels of macroscopicity for large squeezing and numbers of detected photons m [34,35].

In order to enhance the optomechanical interaction strength, a pulsed displacement operation is applied to the optical input before injection into the cavity, resulting in a short pulse of duration τ and total photon number N_p . The displacement can be implemented by admixing a strong coherent field on a highly transmitting (T_{disp}) beam splitter.

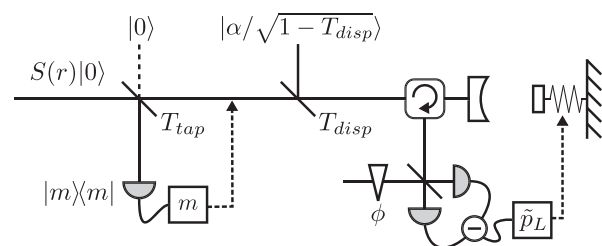


FIG. 1. Employing displaced PSSV states of light as resource for driving a cavity optomechanical QND interaction, the mechanical oscillator is projected into a highly nonclassical state conditioned on the outcome of a subsequent homodyne detection of the optical phase quadrature.

Following the optomechanical interaction, a disentangling homodyne measurement on the reflected optical field projects the mechanics into a highly nonclassical quantum state as detailed in the following.

Optomechanical interaction.—We consider a single-ended cavity optomechanical system with coupling strength g_0 and a mechanical oscillator at frequency ω_M whose period T is much longer than the optical pulse. Furthermore, the cavity bandwidth κ (HWHM) is assumed to be much broader than that of the optical pulse, that is, $\omega_M \ll \tau^{-1} \ll \kappa$. Under these conditions, the dynamics of the optical intracavity field can be adiabatically eliminated and mechanical damping and noise processes can be neglected during the interaction time [31,36]. This leads to input-output relations of the well-known QND form [42],

$$x_L^{\text{in}} \rightarrow x_L = x_L^{\text{in}}, \quad (1a)$$

$$p_L^{\text{in}} \rightarrow p_L = p_L^{\text{in}} + \chi x_M^{\text{in}}, \quad (1b)$$

$$x_M^{\text{in}} \rightarrow x_M = x_M^{\text{in}}, \quad (1c)$$

$$p_M^{\text{in}} \rightarrow p_M = p_M^{\text{in}} + \chi x_L^{\text{in}} + \Omega, \quad (1d)$$

where $x_{L(M)}$ and $p_{L(M)}$ are the conjugate fluctuation quadratures for the light field (mechanical oscillator). We have introduced the coupling strength $\chi = 4g_0\sqrt{N_p}/\kappa$, weighting the contribution of the measured mechanical position x_M^{in} to the optical output phase quadrature, and the associated backaction $\Omega = \chi\sqrt{N_p}/2$ imposed on the mechanical phase quadrature. Through this optomechanical interaction, the motion of the mechanical oscillator becomes correlated with the state of the optical pulse reflected off the cavity.

Performing a postinteraction homodyne measurement of the phase quadrature of the reflected light, p_L , will project the oscillator into a state that inherits features of the input optical state, thereby leading to a partial state transfer from light to mechanics. The actual extent of this imprint depends on the coupling strength and on the amount of mechanical noise. The same QND-type interaction that we use for state transfer can also be used initially to decrease this noise and to do a tomographic characterization of the final mechanical state.

Three-pulse protocol.—In order to accomplish these three tasks, we suggest implementing a three-pulse protocol. The three pulses—precooling, state transfer, and state readout—all happen with precise timing within a single mechanical period as illustrated in Fig. 2. Squeezed vacuum can be produced continuously while the pulsing is implemented by the much stronger displacement beam. The first and the third pulse comprise bright phase squeezed states while the second pulse is a displaced PSSV state. The protocol is successful when the photon subtraction happens in sync with the mechanical motion.

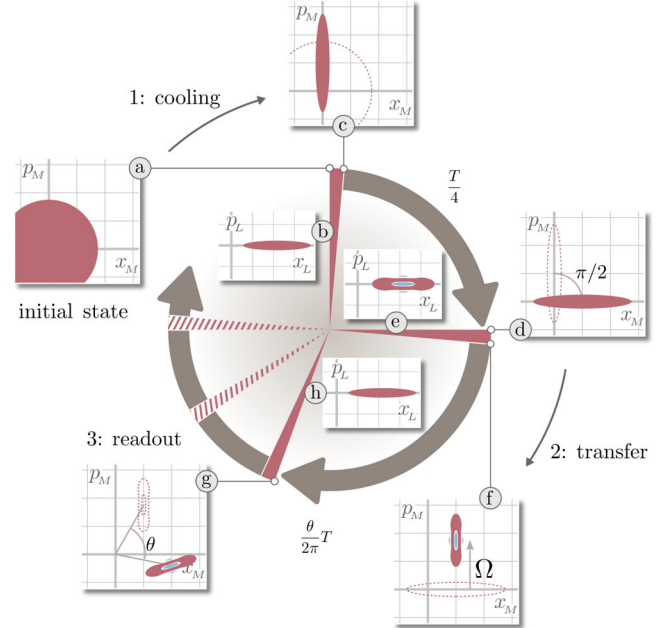


FIG. 2. The three-pulse protocol illustrated on a “clock” corresponding to one mechanical oscillation period, T . Mechanical (optical) states at each protocol sequence are illustrated by the outer (inner) set of Wigner functions. Starting from an initially thermal mechanical state (a) the first pulse of squeezed light (b) cools the mechanics in one quadrature (c). A quarter period later (d), the second pulse transfers the photon-subtracted state (e) onto the mechanics (f). Finally, after a variable interval (g) the third pulse (h) reads out a rotated quadrature of the state. All three QND interactions are accompanied by a homodyne detection of the reflected optical field (not shown).

The first pulse prepares the mechanical oscillator in an asymmetrically cooled state. Even at cryogenic temperatures, the thermal equilibrium state of the relatively low-frequency oscillators needed here will be very noisy and will preclude any direct mapping of nonclassical features from the light, thus necessitating some kind of precooling. Ordinary sideband laser cooling is excluded as we are operating in the unresolved sideband regime, and while optical feedback cooling holds promises for reaching the ground state in the bad-cavity limit as well [43], it still remains to be demonstrated [44]. As an alternative, single quadrature cooling by measurement [32] can be invoked. As can be seen from Eqs. (1a)–(1d), the state preparation process is only affected by the noise of the mechanical momentum variable and it is therefore sufficient to “cool” only that motional degree of freedom. This can be achieved by an initial QND interaction and homodyne detection, after which the variances of the mechanical quadratures will be

$$V_{x_M}^c = \frac{V_{x_M}}{1 + \chi_c^2 V_{x_M}/V_{p_L}}, \quad (2)$$

$$V_{p_M}^c = V_{p_M} + \chi_c^2 V_{x_L}. \quad (3)$$

The position quadrature will thus be cooled near or below the shot-noise level with even moderate interaction strengths. An initial squeezing in the optical p_L quadrature further enhances the cooling.

A quarter period later the reduced noise is transferred to the momentum quadrature by the oscillator's free evolution, cueing the second and principal light-mechanics interaction which effectuates the state preparation. An important point to address is that the actual mechanical state prepared is conditioned on the outcome, \tilde{p}_L , of the homodyne measurement of the reflected light. The state will be displaced along the x_M direction in phase space by an amount proportional to \tilde{p}_L . This displacement does not influence any nonclassical features of the state, but in order to do a tomographic state reconstruction, it is necessary to correct for (using high-speed feedback on the mirror) or keep track of it. It is in principle enough to simply record the displacement values and take these into account in the statistical analysis of the tomographic data [32]. A third option is to condition the state preparation on a homodyne measurement within a narrow acceptance window around $\tilde{p}_L = 0$, in which case the success rate goes down but all mechanical states are created identically. See the Supplemental Material [36] for an analysis of the trade-offs of window size.

Finally, the last pulse is used to read out the mechanical quadratures, again using a QND coupling followed by homodyne detection. For full state tomography, the delay between the second and third pulse is varied in order to map out a range of quadrature phases within a half mechanical period. The resolution of this readout measurement is given by the interaction strength χ and the noise of the optical pulse. It is thus important to note that due to the squeezing of the optical quadrature, the resolution of the measurement is greatly improved compared to the coherent state based protocol proposed in [31] and demonstrated in [32].

The initial states, the displacement operation, the QND interaction and the homodyne detection are all Gaussian, so the full cooling and state-preparation process can advantageously be modeled using standard Gaussian formalism, that is, manipulation of covariance matrices and displacement vectors [37]. The only non-Gaussian operation is the m -photon detection that heralds the nonclassical input light state. This must be modeled by an overlap integral between the Gaussian state and the detector's Wigner function. For a given input light state $W_L^{\text{in}}(x_L, p_L)$ and precooled mechanical state $W_M^{\text{in}}(x_M, p_M)$, the mechanical state prepared from the optomechanical interaction and the homodyne measurement is, up to a normalization factor, obtained by

$$W_M^{\text{out}}(x_M, p_M) = \int \int dx_L dp_L W_L^{\text{in}}(x_L, p_L - \chi x_M) \times W_M^{\text{in}}(x_M, p_M - \chi x_L - \Omega) \delta(p_L - \tilde{p}_L). \quad (4)$$

The state that is actually read out via the optical tomographic measurements will be afflicted by the noise in the third

pulse's p_L quadrature. As seen from (1b), the optical tomogram can be modeled by scaling the mechanical state by a factor χ and convolving with a symmetric Gaussian whose variance is that of the squeezed p_L quadrature. See the Supplemental Material [36] for more details on the model.

Proposed system.—As a feasible system for implementation of the protocol, we propose an optomechanical device merging existing technologies from fiber microcavities [45] with tethered Si_3N_4 membrane mechanical resonators [46]. In this way the pulsed QND condition can be fulfilled while maintaining an appreciable g_0/κ ratio by combining the low frequency and low dissipation mechanical trampoline mode with the small size of the fiber cavity. In particular, we consider an optomechanical Fabry-Perot resonator at $\lambda_L = 1550$ nm consisting of the membrane (patterned with a high-reflectivity photonic crystal) separated $4 \mu\text{m}$ from a concave mirror formed directly at the facet of a fiber. We take the membrane to have mechanical frequency $\omega_M/2\pi = 100$ kHz, effective mass $M = 1$ ng, and quality factor $Q_M = 10^8$, and we assume an optical cavity linewidth of $\kappa/2\pi = 1$ GHz (finesse ≈ 19000). The amplitude of the mechanical zero-point fluctuation is then $x_{\text{zpf}} = 9.1$ fm and the resulting optomechanical single photon coupling rate $g_0/2\pi = 442$ kHz. Consequently, a QND interaction strength of $\chi = 1$ can be achieved using only $N_p = 3.2 \times 10^5$ photons in the input pulse. For the optical state preparation, we will assume $T_{\text{tap}} = 0.98$, $T_{\text{disp}} = 0.999$ and $\eta = 0.8$, and we take the initial mechanical state to be in thermal equilibrium with an environment at temperature $T_{\text{bath}} = 100$ mK.

Examples of the resulting mechanical state Wigner functions W_M^{out} for 1 and 3 subtracted photons, taking $r = 1.15$ (10 dB of squeezing), are plotted in Fig. 3. Along with the actual mechanical states, we also plot the states as they would appear after a tomographic characterization using either coherent state or squeezed state probes. We see that it is indeed possible to obtain signatures of a Schrödinger catlike state, namely two significantly separated components in a coherent superposition as indicated by the negative-valued interference fringes. The readout noise smears out the features of the Wigner function, but it is clearly advantageous to use a squeezed probe as this retains much more of the mechanical state in the optical tomogram.

To assess the “quantumness” of the mechanical states when varying the experimental parameters, we employ a macroscopicity measure [47],

$$\mathcal{I} = -\frac{\pi}{2} \int \int dx dp W(x, p) \left(\frac{\partial^2}{\partial x^2} + \frac{\partial^2}{\partial p^2} + 2 \right) W(x, p). \quad (5)$$

This measure quantifies a state's coherence and extent in phase space through the sharpness of its Wigner function features. It is furthermore directly linked to the state's decoherence rate under simple phonon loss. Finally, for pure states \mathcal{I} is also the number of “nonclassical” phonons in the state, that is, the phonon number minimized over all

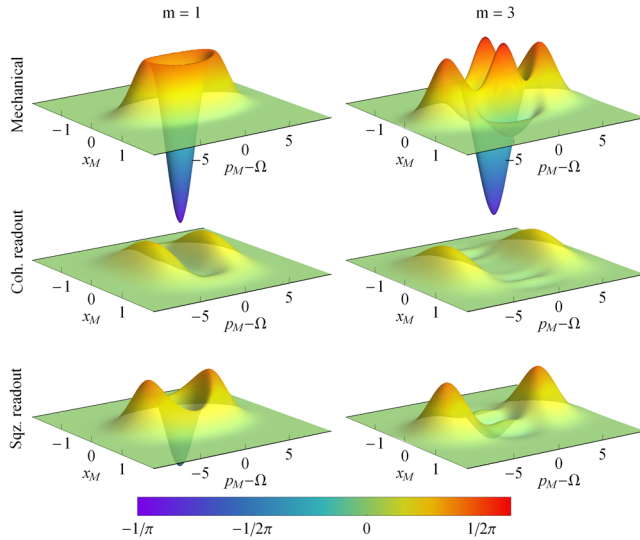


FIG. 3. Wigner function representation of conditionally prepared mechanical states W_M^{out} (top) and corresponding tomographically reconstructed states using coherent (middle) and squeezed light (bottom) readout fields for QND interaction strengths of $\chi = 1$ ($\Omega = 400$). Input PSSV states with $m = \{1, 3\}$, a squeezing strength of $r = 1.15$, and a thermal environment temperature of $T_{\text{bath}} = 100$ mK are assumed. Note the aspect ratio and offset of the phase space coordinates. These are a result of the strong squeezing of the mechanical mode obtained through the QND interaction and of the backaction momentum kick Ω , respectively.

displacement operations. As a point of reference, a pure cat state $|\alpha\rangle \pm |-\alpha\rangle$ with amplitude $\alpha = 2$, which can be said to be a truly macroscopic quantum state [48] has $\mathcal{I} = 4$. Additionally, we look at the total negativity of the Wigner function [49,50], $\mathcal{N} = \int \int dx_M dp_M |W_M^{\text{out}}(x_M, p_M)| - 1$, as a traditional signature of nonclassicality.

We investigate these two figures of merit for the prepared mechanical states with $m = 1, 3$ (corresponding to the top row of Fig. 3) as functions of the optomechanical interaction strength χ . The solid curves of Figs. 4(a) and 4(b) confirm the impression from Fig. 3 that considerable macroscopicity and large negativities are possible even for moderate values of χ .

Of course, in a realistic setting several effects would cause a degradation of the obtainable values of \mathcal{I} and \mathcal{N} . In Fig. 4 we also show the influence of probably the two most critical degrading effects, namely phase fluctuations and optical losses. Stability of the phase space displacement is of high importance as fluctuations will smear out the fine structures of the cat state as can be seen from the dashed and dotted curves. As the effect of the fluctuations are amplified by the magnitude of the displacement they may lead to an optimum value of the QND interaction strength where large coupling is balanced with low smearing. We have modeled both phase and amplitude fluctuations as normally distributed and included them by replacing the coherent state of the displacement beam with an

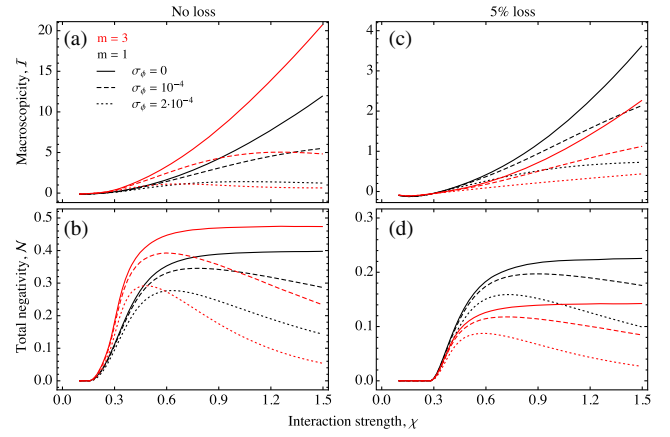


FIG. 4. Macroscopicity (a,c) and total negativity (b,d) of prepared mechanical states as a function of QND interaction strength and impact of displacement field phase fluctuations (standard deviation in radians) and optical loss (c,d) in the input mode. System parameters and assumptions are similar to those of Fig. 3 (top). Displacement amplitude fluctuations are assumed negligible.

asymmetric thermal state [36]. As can be seen, phase fluctuations should be kept near or below 10^{-4} rad on the relevant time scales of the experiment. This will be challenging but should not be impossible to reach with a tight phase lock loop. The influence of amplitude fluctuations is minor compared to that of phase.

With 5% optical losses (modeled by a beam splitter in the path before displacement), macroscopicity and total negativity are decreased as shown in Figs. 4(c) and 4(d), respectively. Since the macroscopicity quantifies a state's susceptibility to decoherence, the initially highly macroscopic state obtained for $m = 3$ subtracted photons is hit particularly hard by losses and the resulting state is in fact less macroscopic than that for $m = 1$. To observe large values of macroscopicity, the losses clearly have to be kept at a minimum. On the other hand, even with losses there is still a significant amount of Wigner function negativity and thus the state remains strongly nonclassical.

Finally, we should point out that the proposed dynamical “cooling” protocol, while sufficient for state preparation alone, must be accompanied by standard passive cooling to mitigate thermal decoherence processes in the system. These should not be significant during a single period of the mechanical oscillator to allow for cooling, preparation, and readout before the quantum state of the system is perturbed by coupling to the environment's thermal noise. Meeting this condition requires both the thermal heating of the precooled mechanical state, occurring at a rate proportional to $\bar{n}_{th}\Gamma_M$, with \bar{n}_{th} being the mean phonon number of the environment and Γ_M the mechanical damping rate, as well as the thermal decoherence of the prepared macroscopic state to be much slower than a mechanical oscillation period. For a true mechanical cat state with component state amplitude $\alpha = 3$, comparable to the

$m = 3$ state in Fig. 3, the decoherence time is $\tau_{\text{dec}} \approx [2\bar{n}_{th}\Gamma_M(1 + 2\alpha^2)]^{-1} \approx 200 \mu\text{s}$ [51] for an environment at 100 mK, and for the system in question, heating out of the motional ground state happens on a time scale of $\tau_{th} = 7.6$ ms. Comparing this to the mechanical oscillation period $\tau_M = 10\mu\text{s}$ we see that the proposed protocol is indeed a viable approach to demonstration of truly macroscopic quantum states of mechanical motion.

Conclusion.—We have presented a protocol for generation of Schrödinger catlike states of a macroscopic mechanical oscillator, relying on previously demonstrated techniques and compatible with existing cavity optomechanical systems. By taking advantage of squeezed-light enhanced quantum nondemolition interactions, non-Gaussian resources, and homodyne detection we have circumvented the demanding requirements of strong single-photon coupling and operation in the sideband resolved regime. Consequently, our results pave a feasible route towards the long-standing goal of interrogating quantum mechanical phenomena at the macroscopic scale.

This work was supported by the Lundbeck Foundation (Grant No. R69-A8249) and Villum Fonden (Young Investigator Programme and Grant No. 13300). We thank Anders S. Sørensen for helpful discussions.

*ulrich.hoff@fysik.dtu.dk

- [1] E. Schrödinger, *Naturwissenschaften* **23**, 807 (1935).
- [2] C. Monroe, D. M. Meekhof, B. E. King, and D. J. Wineland, *Science* **272**, 1131 (1996).
- [3] D. Leibfried, E. Knill, S. Seidelin, J. Britton, R. B. Blakestad, J. Chiaverini, D. B. Hume, W. M. Itano, J. D. Jost, C. Langer, R. Ozeri, R. Reichle, and D. J. Wineland, *Nature (London)* **438**, 639 (2005).
- [4] M. Brune, E. Hagley, J. Dreyer, X. Maître, A. Maali, C. Wunderlich, J. M. Raimond, and S. Haroche, *Phys. Rev. Lett.* **77**, 4887 (1996).
- [5] S. Deléglise, I. Dotsenko, C. Sayrin, J. Bernu, M. Brune, J.-M. Raimond, and S. Haroche, *Nature (London)* **455**, 510 (2008).
- [6] G. Kirchmair, B. Vlastakis, Z. Leghtas, S. E. Nigg, H. Paik, E. Ginossar, M. Mirrahimi, L. Frunzio, S. M. Girvin, and R. J. Schoelkopf, *Nature (London)* **495**, 205 (2013).
- [7] B. Vlastakis, G. Kirchmair, Z. Leghtas, S. E. Nigg, L. Frunzio, S. M. Girvin, M. Mirrahimi, M. H. Devoret, and R. J. Schoelkopf, *Science* **342**, 607 (2013).
- [8] J. S. Neergaard-Nielsen, B. M. Nielsen, C. Hettich, K. Mølmer, and E. S. Polzik, *Phys. Rev. Lett.* **97**, 083604 (2006).
- [9] A. Ourjoumtsev, H. Jeong, R. Tualle-Brouiri, and P. Grangier, *Nature (London)* **448**, 784 (2007).
- [10] K. Huang, H. Le Jeannic, J. Ruaudel, V. B. Verma, M. D. Shaw, F. Marsili, S. W. Nam, E. Wu, H. Zeng, Y.-C. Jeong, R. Filip, O. Morin, and J. Laurat, *Phys. Rev. Lett.* **115**, 023602 (2015).
- [11] S. Mancini, V. I. Man'ko, and P. Tombesi, *Phys. Rev. A* **55**, 3042 (1997).
- [12] S. Bose, K. Jacobs, and P. L. Knight, *Phys. Rev. A* **56**, 4175 (1997).
- [13] U. Akram, W. P. Bowen, and G. J. Milburn, *New J. Phys.* **15**, 093007 (2013).
- [14] R. Ghobadi, S. Kumar, B. Pepper, D. Bouwmeester, A. I. Lvovsky, and C. Simon, *Phys. Rev. Lett.* **112**, 080503 (2014).
- [15] M. Paternostro, *Phys. Rev. Lett.* **106**, 183601 (2011).
- [16] M. R. Vanner, M. Aspelmeyer, and M. S. Kim, *Phys. Rev. Lett.* **110**, 010504 (2013).
- [17] Y.-D. Wang and A. A. Clerk, *Phys. Rev. Lett.* **108**, 153603 (2012).
- [18] R. Filip and A. A. Rakhubovsky, *Phys. Rev. A* **92**, 053804 (2015).
- [19] A. A. Rakhubovsky, N. Vostrosablin, and R. Filip, *Phys. Rev. A* **93**, 033813 (2016).
- [20] O. Romero-Isart, A. C. Pflanzer, M. L. Juan, R. Quidant, N. Kiesel, M. Aspelmeyer, and J. I. Cirac, *Phys. Rev. A* **83**, 013803 (2011).
- [21] S. G. Hofer, W. Wiczorek, M. Aspelmeyer, and K. Hammerer, *Phys. Rev. A* **84**, 052327 (2011).
- [22] W. Marshall, C. Simon, R. Penrose, and D. Bouwmeester, *Phys. Rev. Lett.* **91**, 130401 (2003).
- [23] A. Carlisle, H. Kwon, H. Jeong, A. Ferraro, and M. Paternostro, *Phys. Rev. A* **92**, 022123 (2015).
- [24] F. Khalili, S. Danilishin, H. Miao, H. Müller-Ebhardt, H. Yang, and Y. Chen, *Phys. Rev. Lett.* **105**, 070403 (2010).
- [25] P. Sekatski, M. Aspelmeyer, and N. Sangouard, *Phys. Rev. Lett.* **112**, 080502 (2014).
- [26] J. S. Bennett, K. Khosla, L. S. Madsen, M. R. Vanner, H. Rubinsztein-Dunlop, and W. P. Bowen, *New J. Phys.* **18**, 053030 (2016).
- [27] T. J. Milburn, M. S. Kim, and M. R. Vanner, *Phys. Rev. A* **93**, 053818 (2016).
- [28] B. Julsgaard, J. Sherson, J. I. Cirac, J. Fiurášek, and E. S. Polzik, *Nature (London)* **432**, 482 (2004).
- [29] P. Marek and R. Filip, *Phys. Rev. A* **81**, 042325 (2010).
- [30] V. B. Braginsky, Y. I. Vorontsev, and F. Y. Khalili, *JETP Lett.* **27**, 276 (1978).
- [31] M. R. Vanner, I. Pikovski, G. D. Cole, M. Kim, C. Brukner, K. Hammerer, G. J. Milburn, and M. Aspelmeyer, *Proc. Natl. Acad. Sci. U.S.A.* **108**, 16182 (2011).
- [32] M. R. Vanner, J. Hofer, G. D. Cole, and M. Aspelmeyer, *Nat. Commun.* **4**, 2295 (2013).
- [33] M. Dakna, T. Anhut, T. Opatrný, L. Knöll, and D.-G. Welsch, *Phys. Rev. A* **55**, 3184 (1997).
- [34] U. L. Andersen and J. S. Neergaard-Nielsen, *Phys. Rev. A* **88**, 022337 (2013).
- [35] A. Laghaout, J. S. Neergaard-Nielsen, and U. L. Andersen, *Opt. Commun.* **337**, 96 (2015).
- [36] See Supplemental Material at <http://link.aps.org/supplemental/10.1103/PhysRevLett.117.143601>, which includes Ref. [37–41], for further details on the optomechanical QND interaction and the generated mechanical state Wigner function.
- [37] A. Ferraro, M. G. A. Paris, and S. Olivares, *Gaussian States in Quantum Information* (Bibliopolis, Napoli, 2005).
- [38] K. Mølmer, *Phys. Rev. A* **73**, 063804 (2006).
- [39] U. L. Andersen and R. Filip, in *Progress in Optics Volume 53*, edited by E. Wolf (Elsevier, New York, 2009), pp. 365–414.

- [40] C. Weedbrook, S. Pirandola, R. García-Patrón, N. J. Cerf, T. C. Ralph, J. H. Shapiro, and S. Lloyd, *Rev. Mod. Phys.* **84**, 621 (2012).
- [41] L. B. Madsen and K. Mølmer, in *Quantum Information with Continuous Variables of Atoms and Light*, edited by N. J. Cerf, G. Leuchs, and E. S. Polzik (Imperial College Press, London, 2007), pp. 435–462.
- [42] P. Grangier, J. A. Levensen, and J.-P. Poizat, *Nature (London)* **396**, 537 (1998).
- [43] C. Genes, D. Vitali, P. Tombesi, S. Gigan, and M. Aspelmeyer, *Phys. Rev. A* **77**, 033804 (2008).
- [44] D. J. Wilson, V. Sudhir, N. Piro, R. Schilling, A. Ghadimi, and T. J. Kippenberg, *Nature (London)* **524**, 325 (2015).
- [45] N. E. Flowers-Jacobs, S. W. Hoch, J. C. Sankey, A. Kashkanova, A. M. Jayich, C. Deutsch, J. Reichel, and J. G. E. Harris, *Appl. Phys. Lett.* **101**, 221109 (2012).
- [46] R. A. Norte, J. P. Moura, and S. Gröblacher, *Phys. Rev. Lett.* **116**, 147202 (2016).
- [47] C.-W. Lee and H. Jeong, *Phys. Rev. Lett.* **106**, 220401 (2011).
- [48] H. Jeong, A. P. Lund, and T. C. Ralph, *Phys. Rev. A* **72**, 013801 (2005).
- [49] A. Kenfack and K. Yczkowski, *J. Opt. B* **6**, 396 (2004).
- [50] D. Kleckner, I. Pikovski, E. Jeffrey, L. Ament, E. Eliel, J. van den Brink, and D. Bouwmeester, *New J. Phys.* **10**, 095020 (2008).
- [51] M. S. Kim and V. Bužek, *Phys. Rev. A* **46**, 4239 (1992).